Time dependency of compression behaviour for methane hydrate bearing sand

Shintaro Kajiyama[1], M. Hyodo[1], Y. Nakata[1], N. Yoshimoto[1],
K. Nakashima[1], and S. Hiraoka[1]

[1] Graduate school of Sciences and Technology for Innovation, Yamaguchi University, 2-16-1, Tokiwadai, Ube City 755-8611, Japan.

ABSTRACT

In this study, the time dependency of methane hydrate (hereafter referred to as MH) bearing sand is investigated by changing the loading rate and effective stress on two types of artificial MH bearing sand. From the results, it was revealed that the axial strain under constant effective stress decreased power functionality with time, regardless of the existence of MH, at any effective stress. A longer time was required to increase the decrement of the void ratio than that of the host sand and the decrement of the void ratio tended to be larger in the host sand than that of MH bearing sand. When the difference in the change of the void ratio between MH bearing sand and that of the host sand under a constant effective stress was compared, it became obvious that a larger fines content led to a larger difference.

Keywords: methane hydrate; time dependency; compression

1 INTRODUCTION

Recently, research and development related to MH is being conducted in order to prepare for its production in Japan. In fact, in 2017, 2nd offshore production test in the Nankai Trough was carried out in order to investigate the viability of methane gas extraction from the sea bed for commercial purposes (MH21 Research Consortium). MH exists as a solid in the voids of sand in that site. For well drilling to recover MH as methane gas (hereafter referred to as MH production), it is necessary to study the stability of the wells and the risks to the environment of the sea bed due to the change of stress conditions in the ground. MH production is mainly performed using a depressurizing method, in which the MH layer is depressurized to a point outside of its stability region. The geology of the Nankai Trough is formed by sand and muddy layers called turbidite, MH is concentrated in the sand layers, and a wide grain size distribution exists in the MH rich layers. A series of triaxial shear tests have been performed on artificial MH bearing sands (Hyodo et al., 2013; Kajiyama et al., 2017). However, it is assumed that the production of MH will be a long-term procedure. Fig.1 schematically shows the effective stress and elapsed time of MH bearing sand over time during MH production. This figure shows the above-mentioned underground stress changes not only during excavation but also during MH production over a long term. In addition, not only the physical properties are changed due to the MH decomposition of MH bearing sand but also pressure propagation will gradually occur, so it is considered that the stress changes with time even in the state of MH bearing sand (from the blue plot to the red plot in Fig. 1). However, few studies on the time dependency of MH bearing sand are present (Miyazaki et al., 2009), but this property is an important characteristic for MH long-term production. In this study, in order to grasp the mechanical behavior of an MH layer from the start of MH production to the start of dissociation of MH, the time dependence of MH bearing sand by changing the effective stress and loading rate applied to MH bearing sand is investigated.

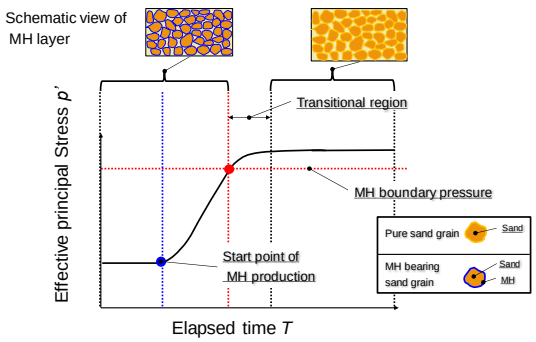

Fig.1 Schematic view of effective stress and elapsed time of MH bearing sand over time during MH production

2 TESTING APPARATUS

The temperature-controlled high pressure triaxial testing apparatus was developed such that the back pressure and confining pressure could be controlled under various temperature and high pressure conditions in order to examine the mechanical behaviour of MH bearing sand specimens under deep seabed stress and temperature conditions (Hyodo et al., 2013). Cell pressure can be applied up to 30MPa. Pore pressure can be controlled in the range of 0MPa to 20MPa. Calculation of the methane gas was performed using a gas mass flow meter. Temperature was controlled by a system which circulated the cell fluid from a low temperature water tank set up outside allowing the temperature to be adjusted from -20ºC to +50ºC. The temperature measurement during the experiment is carried out by a thermocouple installed in the triaxial chamber.

3 MATERIAL AND SAMPLE PREPARATION

In this study, the samples were simulated to mimic the grain size distribution and mineral composition of the MH rich layer. The minerals and mixing ratio are shown in Table 1. Hereafter material with low fines content is called AS1 and the other is referred to as AS2. The grain size distribution of the MH simulated sample used in this study is shown in Fig. 2. The shaded part in Fig. 2 shows the width of the grain size distribution of the MH rich layer of the Nankai Trough. During preparation of the specimen, the water content was adjusted in advance to a target MH saturation S_{MH} (%), so as to have a predetermined density in a mold having a diameter of 30mm and a height of 60mm using the wet tamping method. In this study, frozen specimens were used.

4 TESTING CONDITION AND PROCEDURE

After forming the specimen, it was subjected to a series of processes under specific temperatures and pressures. First of all, the specimen was installed in the triaxial cell. Next, the back pressure was increased to 4MPa while methane was injected into the specimen by filling the pores of the specimen with methane. Then, the frozen specimen was thawed to a temperature outside of the MH stability zone inside the tri-axial cell.

Table 1. Blending table of simulated samples

	No.7 silica	No.8 sillica	R5.5 sillica	Kaolin	MK-300 mica
AS1 (%)	70	17	10	1	2
AS2 (%)	30	55	7	3	5

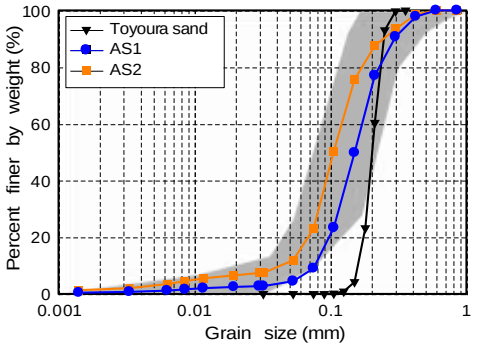

Fig.2 Grain size distribution curves

Next, the temperature in the triaxial cell was lowered to 1ºC so that the MH could be stable. By keeping the gas pressure constant in the connection between the specimen and the syringe pump and by observing the amount of gas flowing at various times, the transformation of water within the pores into hydrate was judged to be complete if there was no marked change.

After the hydrate was generated, water under constant pressure was allowed to infiltrate the specimen. Then, the pore water pressure was applied and the temperature was adjusted to the prescribed test condition. While keeping the pressure constant, consolidation was carried out until the specified effective stress was reached. In the test, the following three kinds of experiments were conducted. 1: Incremental loading test in which the effective stress was held for 1 hour each time the effective stress is increased. 2: A monotonic test with monotonous loading until reaching a specified stress, and then holding the stress for the same time as the time required for the incremental loading test. 3: Consolidation test in which consolidation was terminated at a time designated using the 3t method after monotonic loading. After testing, the temperature in the specimen was increased and MH dissociated; the amount of gas was measured using the gas mass flow meter. The amount of gas measured was then converted into MH saturation.

Table 2. Test condition

Case No.	Name of Host material	Fines content (%)	Degree of Saturation by MH* S_{MH} (%)	Back Pressure B.P.(MPa)	Effective Confining Presuure σ_c' (MPa)	Cell Presuure σ_c (MPa)	Temperture T(°C)	Specific Density ρ_s(g/cm^3)	Void ratio e	Porosity n(%)	Consolidation condition
1	AS1	8.9	0 (Host sand)	10	1.0	11.0	20	2.66	0.822	45.1	3t method
2					3.0	13.0	20		0.828	45.3	3t method
3					5.0	15.0	20		0.817	45.0	3t method
4			63.3		7.0	12.0			0.812	44.8	Monotonic loading
5			40.5		14.0	19.0			0.796	44.3	Incremental loading
6			47.4	10	1.0	11.0	5	2.66	0.828	45.3	3t method
7			48.8		3.0	13.0			0.821	45.1	3t method
8			-		5.0	15.0			0.850	45.9	3t method
9	AS2	22.9	0 (Host sand)	10	3.0	3.0	20	2.67	0.771	43.5	3t method
10			49.4	10	3.0	13.0	5	2.67	0.835	45.5	3t method

* Target Degree of Saturation by MH is 50%

5 TIME DEPENDENCY DURING ISOTROPIC CONSOLIDATION TEST

In this study, with consideration given to the thickness of sedimentary layers above the MH layer and that MH production is carried out by the depressurization method, consolidation stress was set at 1, 3, 5, 7 and 14MPa. Table 2. shows a list of test results used in this study. Regarding Case 8, since it was not possible to measure the amount of gas, it is considered to be approximately 50%. Fig. 3 shows the relationship between effective stress and elapsed time during consolidation of each case from Case 1 to Case 8. Regarding the results of the effective stress of 5MPa for host sand, it could not be recorded until the effective stress reached 3.3MPa, at which point the measurement results started recording. Fig. 4 shows the relationship between the void ratio difference Δe from the start of consolidation to the end of consolidation and the elapsed time. In all of the samples, it can be seen that when the predetermined effective stress is reached and the process proceeds to the stress holding process, the change in amount of the void ratio decreases and changes with time. Fig. 5 shows the relationship between the void ratio difference Δe from the beginning of consolidation and effective stress. Comparing the amount of difference of void ratio between the monotonic loading and the incremental loading at the effective stress of 7MPa, it is clear that the variation of the void ratio of monotonic loading is larger than that of incremental loading. On the other hand, when the consolidation test was terminated by the 3t method, it became clear that the creep deformation of MH bearing sand is larger than that of host sand at any effective stress in comparison between each effective stress. Also, referring to the loading speed in Fig. 3 and comparing Case 1 and Case 6, it is clear that the void ratio difference during loading is small despite almost the same loading speed. So it is clear that the time dependence of MH bearing sand is larger than that of the host sand. In addition, when comparing Case 4, Case 5 and Case 6, it is obvious that the amount of change in the void ratio during loading is smaller as the loading speed becomes larger, so the time dependence by the loading speed of MH bearing sand becomes clear. Fig. 6 shows the relationship between the axial strain rate (ε_a/min) during the experiment and the elapsed time. Regardless of any effective stress, it is understood that the axial strain rate linearly decreases on the logarithmic graph when reaching the target effective stress with or without MH. From this, it was found that the axial strain at creep decreases power functionally with time. In addition, it is clear that, compared with each effective stress, the initial axial strain rate increases with increasing the effective stress with or without MH.

Fig. 7 shows the relationship between the difference of the void ratio and the elapsed time from the time

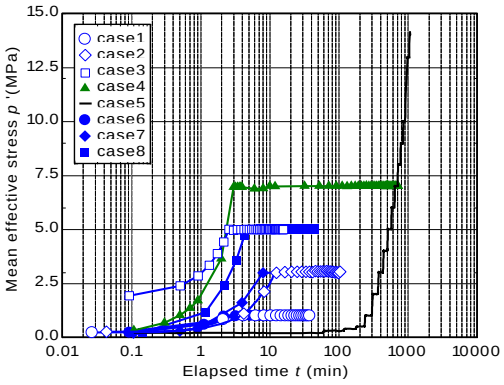

Fig.3 Relationship between effective stress and elapsed time during experiment

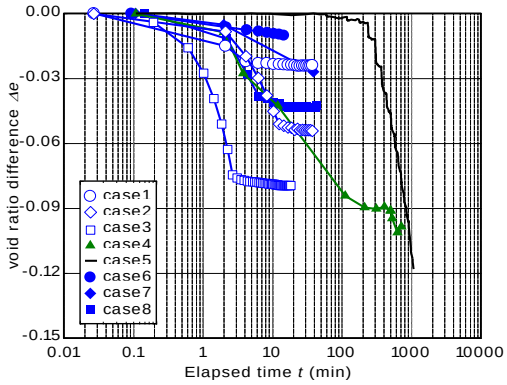

Fig.4 Relationship between the void ratio difference at the start of consolidation and elapsed time

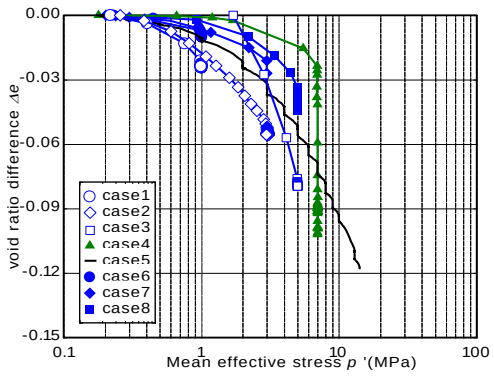

Fig.5 Change in effective stress and void ratio from the start of consolidation

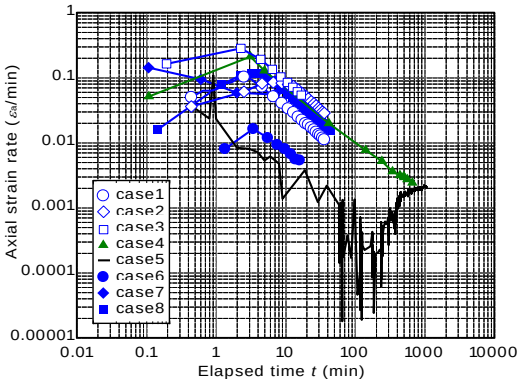

Fig.6 Relationship between axial strain rate and elapsed time

when the predetermined effective stress 3MPa is reached in the test on AS1. From the figure, after the effective stress become constant, it is found that the decrement of void ratio increases with increasing the effective stress with or without MH. Furthermore, with or without MH, the decrement of the void ratio linearly changes after a certain time has elapsed. In addition, compared with the presence or absence of MH, although it is almost unchanged at 1MPa, there is a tendency that the time for the amount of decrease in void ratio of MH bearing sand beginning to increase is longer than that of the host sand and the decrease ratio of the void ratio of MH bearing sand is larger that of the host sand. A similar tendency was also observed in the consolidation test results of MH bearing sand carried out using Toyoura sand (Miyazaki et al., 2009), and it is inferred that MH has a time dependence regardless of the presence or absence of fines. Fig. 8 shows the relationship between the change in the void ratio of AS1 and AS2 and time after the effective stress has reached 3MPa. From the figure, it is clear that when the host sands are compared with each other, the void ratio difference is larger when the fines content is larger. Comparing the difference between the MH bearing sand and the host sand in each sample, the difference between AS2 with a large amount of fines contents is larger. From this result, it is suggested that the time dependence becomes more conspicuous when MH bearing sand has large fines contents. Since MH production is assumed to be long-term, it is suggested that these time dependencies become more important as the production may be carried out for years.

6 CONCLUSIONS

In this study, MH was generated for a simulated sample of the Nankai Trough, and a consolidation test was conducted by changing effective stress and loading rate. Conclusions are summarised as follows:

(1) When comparing the same effective stresses, creep deformation of MH bearing sand is larger than that of host sand. In addition, the larger the loading speed of the MH bearing sand, the smaller the change in the void ratio during loading.

(2) At any effective stress, with or without MH, the axial strain under constant effective stress decreases power functionally with time.

(3) Under a constant effective stress, the time dependence of the increment of the void ratio becoming large with the passage of a certain time was recognised. There is a tendency that the time for the amount of decrease in void ratio of MH bearing sand beginning to increase is longer than the host sand, and the decrease ratio of the void ratio of MH bearing sand is larger that of the host sand. This tendency is more conspicuous as the fines content becomes larger.

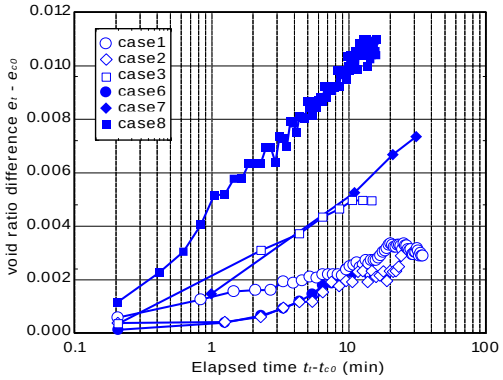

Fig.7 Relationship between the void ratio difference due to difference in effective stress and elapsed time from the start of stress retention

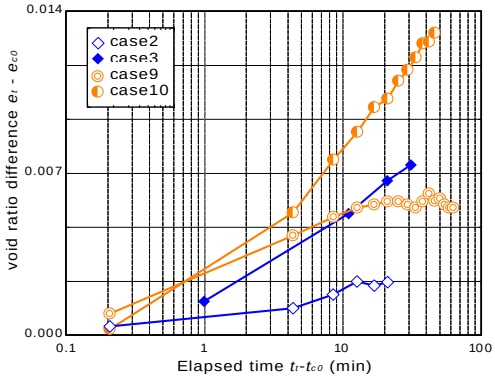

Fig.8 Relationship between the amount of void ratio difference due to difference in fines content and elapsed time from the start of stress retention

ACKNOWLEDGEMENTS

This work was supported by funding from the Research Consortium for Methane Hydrate Resources in Japan (MH21 Research Consortium) planned by the Ministry of Economy, Trade, and Industry (METI), Japan. And part of this work was supported by JSPS KAKENHI Grant Number JP 17H06899.

REFERENCES

Hyodo, M., Yoneda, J., Yoshimoto, N., Nakata, Y. (2013). Mechanical and dissociation properties of methane hydrate-bearing sand in deep seabed, Soils and Foundations, 53(2) 299-314.

Kajiyama, S., Hyodo, M., Nakata, Y., Yoshimoto, N., Wu, Y., Kato A. (2017). Shear behaviour of methane hydrate bearing sand with various particle characteristics and fines, Soils and Foundations, 57(2), 176-193.

MH21 Reserch Consortium, Information about the Second Offshore Production Test, (2018).
http://www.mh21japan.gr.jp/english/infomation/976/

Miyazaki, K., Yamaguchi, T., Sakamoto, Y., Haneda, H., Ogata, Y., Aoki, K., Okubo, S. (2009). Creep of Sediment Containing Synthetic Methane Hydrate, Journal of MMIJ 125, 156-164.